Freely assembled multifunctional acoustofluidic devices based on flexible printed circuit boards

Shaoshuai Han, Di Lian, Linjin Wu, Boyu Zhao, Jiayang Wang, Yi Fang, Peiyao An, Ning Li, Yue Li, Jun Ren, Dongfang Liang, Xin Yang, Zhenlin Wu

Abstract— Surface acoustic wave (SAW) based acoustofluidics has demonstrated strong potential in micro- and nanoparticle manipulation, including applications such as acoustic centrifugation and particle patterning. However, conventional SAW device fabrication using photolithography and metal deposition is limited by high cost, long processing time, and the inability to modify the structure after fabrication. In this study, a functionally tunable SAW acoustofluidic device based on a flexible printed circuit board (FPCB) is proposed. By mechanically clamping interdigital electrodes (IDEs) on the FPCB to a piezoelectric substrate and incorporating a matching network, efficient SAW excitation is achieved. The device enables rapid enrichment of polystyrene (PS) particles ranging from 500 nm to 5 μm. In addition, controlled patterning of 10 μm particles is realized using a magnetically attached rotating fixture, which allows adjustment of the acoustic wave propagation direction on the substrate to excite different acoustic wave modes. This modular and reconfigurable FPCB-SAW platform provides a cost-effective and adaptable solution for rapid functional validation of SAW devices, supporting the broader application of acoustofluidic systems.

Index Terms— Acoustofluidics, droplet, flexible printed circuit board (FPCB), interdigital electrode (IDE), surface acoustic wave (SAW).

I. Introduction

Surface acoustic wave (SAW)-based acoustofluidic has been widely applied in acoustic centrifugation [1], particle patterning [2], sorting/separation [3], [4], and droplet manip-ulation [5], owing to its advantages of non-contact oper-ation, high precision, and strong integrability [6]. Among various piezoelectric materials, lithium niobate is the most commonly used substrate for SAW devices due to its high electromechanical coupling coefficient [7], [8]. Conventional SAW devices are typically fabricated on lithium niobate substrates using photolithography and defined as interdigitated transducers (IDTs). This process involves multiple cleanroom steps, including mask manufacturing, photoresist spin-coating, mask alignment, UV exposure, metal layer deposition, and lift-off [9]. During the development stage, optimizing structural parameters and addressing inevitable fabrication errors often hinder the immediate achievement of the desired device functionality, thereby extending the development cycle. Currently, the average cost of outsourcing the fabrication of a 4-inch lithium niobate SAW device is approximately USD 700. Once fabricated, the SAW device is fixed, and any modification requires a full redesign, outsourcing, and repeated testing.

Previous studies have demonstrated that different acoustic wave modes and even hybrid acoustic fields can be excited by varying the wafer rotation of lithium niobate [10], [11]. In particular, dual-wave mixing modes generated at optimized crystal phase angles have been shown to significantly enhance particle manipulation performance. However, iterative opti-mization of chip design through lithographic processes sub-stantially increases research and development costs. Therefore, there is an urgent need for a SAW device fabrication approach that is both easily reconfigurable and allows for adjustable wafer rotation.

In this study, a functionally tunable SAW device integrated with a flexible PCB (FPCB-SAW) is proposed. The use of a magnetic pressure assembly enables easy disassembly and reassembly of the SAW device. Electrical characterization experiments confirm that the FPCB-SAW device exhibits strong coupling with radio frequency (RF) signals. The device effectively functions as an acoustic centrifuge, enabling the rapid enrichment of polystyrene microspheres with diameters of 5 μm, 1 μm, and 500 nm. Furthermore, the device was employed to evaluate particle patterning performance under different wafer rotation angles. This technology holds promise for widespread adoption and significantly reduces the development time and cost associated with SAW device fabrication.

II. DEVICE DESIGN AND FABRICATION

In the FPCB-SAW device, a 128° YX-cut $LiNbO_3$ wafer (3 inches in diameter and 0.5 mm thick) was first placed on a 3D-printed supporting plate, as shown in Fig. 1(a). A 10 mm-wide iron ring was nested around the periphery of the wafer, and the magnetic cylindrical components of the

Shaoshuai Han, Di Lian, Linjin Wu, Boyu Zhao, Jiayang Wang, Yi Fang, Peiyao An and Zhenlin Wu are with the School of Optoelectronic Engineering and Instrumentation Science, Dalian University of Technol-ogy, Dalian 116024, China.

Ning Li and Yue Li are with the Department of Dalian Women and Children's Medical Group, Dalian 116024, China

Jun Ren is with the Department of Liaoning Key Laboratory of Molecular Recognition and Imaging, School of Bioengineering, Dalian University of Technology, Dalian, 116024, China

Dongfang Liang is with the Department of Engineering, University of Cambridge, Cambridge CB2 1PZ, UK

Xin Yang is with the Department of Electrical and Electronic Engineering, School of Engineering, Cardiff University, Cardiff CF24 3AA, U.K.

This work was supported in part by the Fundamental Research Funds for the Central Universities under Grant DUT24YG140.

Corresponding authors: Xin Yang, email: yangx26@cardiff.ac.uk, Zhenlin Wu, email:zhenlinwu@dlut.edu.cn

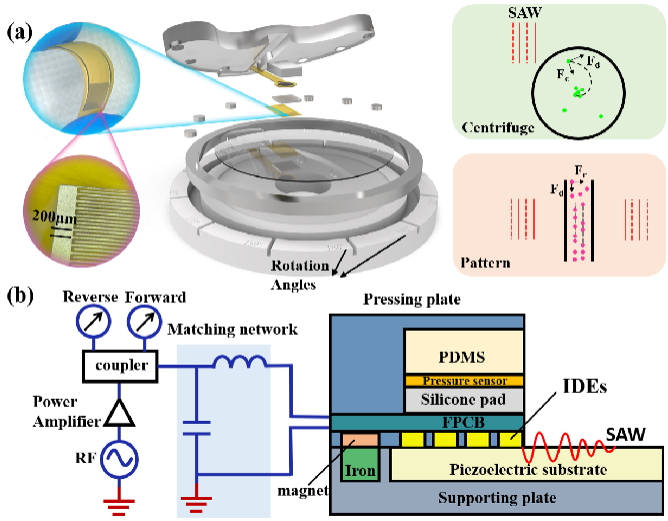

Fig. 1. (a) Magnetically clamped, reconfigurable acoustofluidic device enabling both acoustic centrifugation and particle patterning. (b) Cross-sectional view of the device assembly featuring an integrated impedance matching circuit.

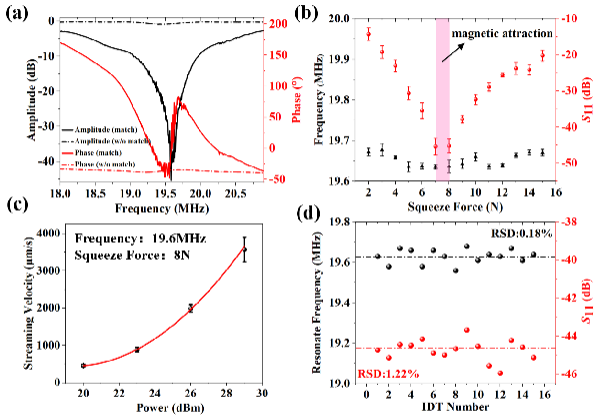

Fig. 2. (a) Amplitude and phase of the S_{11} of the acoustofluidics device with and without the impedance matching network. (b) Relationship between the resonant frequency and S_{11} of the IDT and the clamping force. (c) Relationship between input signal power and streaming veloc-ity in the droplet. 10 μm polystyrene particles were used as tracers. (d) Uniformity test of the acoustofluidic device using FPCBs from the same production batch.

pressing plate provided the clamping force for the FPCB. The FPCB was fabricated using a standard PCB manufacturing process, in which interdigital electrodes (IDEs) composed of a metal bilayer (Au/Cu, 25 μm/18 μm) were patterned onto a 50 μm-thick polyimide film. The IDEs have two electrode periods, 200 μm and 400 μm, and consist of 30 pairs of finger electrodes, each with an aperture size of 20 mm. To address signal coupling issues, the clamped acoustofluidic device was equipped with an impedance matching circuit, as shown in Fig. 1(b) [12]. During operation, forward and reflected power were continuously monitored using two power meters. Different functionalities of the acoustofluidic device were achieved by using different PDMS structures, as described in previous studies [11], [12].

The reflection coefficient S_{11} was measured using a vec-tor network analyzer (LibreVNA, China), as shown in Fig. 2(a). After impedance matching, S_{11} dropped from -2 dB to –46 dB, and the phase approached zero, indicating excellent RF coupling performance. Different clamping forces were applied using a screw-based fixture to evaluate their effects on the resonant frequency and the minimum S_{11} value, and to determine the optimal pressure range for the magnetic assembly. The results indicate that the device achieves the best coupling performance of RF signal when the clamping force is in the range of 7–8 N, as shown in Fig. 2(b). Under the optimal clamping force condition, the influence of different input powers on streaming velocity was studied, as shown in Fig. 2(c), where the velocity was represented by the movement speed of 10 μm PS particles. To evaluate the uniformity of the packaged devices, FPCBs from the same production batch were assembled and their S_{11} parameters were measured, as shown in Fig. 2(d). The relative standard deviation of the resonant frequency was found to be 0.18%, and that of the minimum S_{11} was 1.22%, indicating that the packaging method used in this study ensures good device uniformity.

RESULTS AND DISCUSSION A.

Applications of acoustofluidic centrifuges

FPCB-SAW devices have a wide range of applications, including acoustofluidic centrifugation, particle patterning. Among them, the acoustic streaming centrifuge can be used to verify the effectiveness of acoustic waves in driving acoustic streaming in the clamped device [14]. A PDMS micro-ring with a diameter of 8 mm was added to the central region of the clamped device, with its structure and position based on previous research [11]. According to Fig. 3(a), the acoustic energy of a SAW is radiated at the Rayleigh angle ($\vartheta \approx 22°$ using Snell's law: $(\sin^{-1}(c_f / c_s))$, where c_s and c_f is the speed of sound in the subtrate and the fluid, respectively). Under the action of acoustic waves coupled into the droplet, an acoustic streaming-induced low-pressure region forms at the center of the droplet, driving particles to accumulate at that location, as shown in Fig. 3(b). To evaluate the performance of the acoustofluidic centrifuge, PS particles with diameters of 5 μm, 1 μm, and 500 nm were tested, as shown in Fig. 3(c)–(e). The results demonstrate that all three particle sizes achieved significant enrichment. These experiments confirm that the clamping-based IDT device ensures effective acoustic coupling and promotes strong acoustic streaming, making it suitable for integration in acoustofluidic centrifuge applications.

B. Applications of patterning

The patterning capability of the FPCB-SAW device was further validated using 10 μm particles. In this experiment, 10 μm polystyrene particles were introduced into a microchan-nel measuring 400 μm in width and 40 μm in height. Si-multaneous excitation of opposing IDTs by identical RF signals generated standing acoustic waves in the channel, leading to particle aggregation at pressure nodes, as shown in Fig. 4(a). The device enables free adjustment of sound wave propagation on the piezoelectric substrate to generate different wave modes. S_{11} results after impedance matching

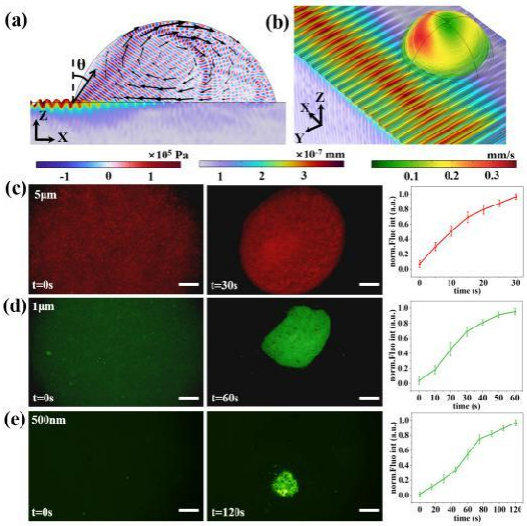

Fig. 3. (a) Coupling mechanism of acoustic waves in microdroplets at 20 MHz in clamped device. (b) Acoustic streaming distribution induced by the IDT on microdroplets. FPCB-SAW device enables rapid concen-tration of PS particles with diameters of (c) 5 μm, (d) 1 μm, and (e) 500 nm, accompanied by normalized fluorescence intensity curves at various concentration times. Scale bar: 50 μm

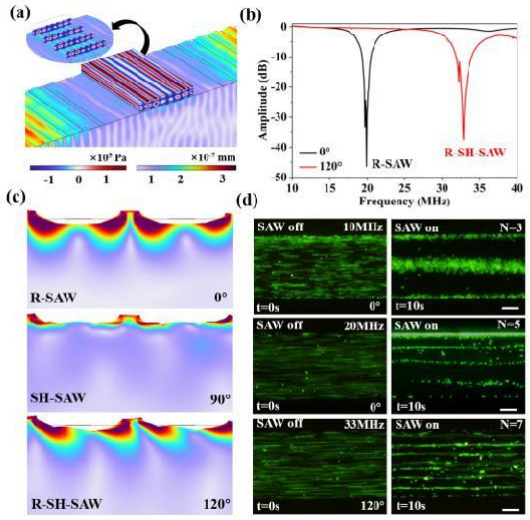

Fig. 4. (a) Acoustic pressure distribution in the microchannel of the FPCB-SAW device aligned with the IDT layout. (b) S_{11}) spectra of the FPCB-SAW device at various crystal orientation angles of the piezo-electric substrate. (c) Acoustic wave modes distribution under different propagation directions. (d) Controlled patterning of 10 μm particles achieved by applying FPCBs with different aperture sizes and exciting acoustic waves along distinct directions. Scale bar: 100 μm

at different angles are shown in Fig. 4(b). At 0°, Rayleigh waves dominate, whereas at 120°, the resonance shifts to 33 MHz, and shear horizontal waves are introduced alongside Rayleigh waves. The influence of these acoustic modes was analyzed using two-dimensional simulation, as shown in Fig. 4(c). By employing a hybrid acoustic field excited under different electrode periods (200 μm and 400 μm) and different wafer rotation angles, the device achieved precise particle arrangement patterns with controllable spacing. The hybrid acoustic field improved spatial control, indicating the device's potential for rapid prototyping and functional validation in SAW-based device research.

IV. CONCLUSION

This paper presents a functionally controllable acoustoflu-idic device based on FPCBs. The FPCB-SAW device matches the performance of traditional photolithography-fabricated counterparts while offering reduced manufacturing costs and simplified assembly. By exploiting the mechanical flexibil-ity, lightweight nature, and compactness of FPCBs, this ap-proach significantly shortens development time and lowers costs for acoustofluidic device fabrication. Functional vali-dation through acoustic centrifugation and microparticle pat-terning demonstrates performance comparable to conventional photolithography-based devices. This technology can greatly promote the popularization of acoustofluidic applications.

REFERENCES

[1] P. Dumcius, R. Mikhaylov, X.Y. Zhang et al., "Dual-Wave Acoustoflu-idic Centrifuge for Ultrafast Concentration of Nanoparticles and Ex-tracellular Vesicles," Small, vol. 19, no. 35, pp. 2300390, 2023, doi: 10.1002/smll.202300390.
[2] P. Vachon, S. Merugu, J. Sharma et al., "Microfabricated acoustofluidic membrane acoustic waveguide actuator for highly localized in-droplet dynamic particle manipulation," Lab Chip, vol. 23, no. 7, pp. 1865-1878, 2023, doi: 10.1039/d2lc01192a.
[3] N. Hao, Z. Wang, P. Liu et al., "Acoustofluidic multimodal diagnostic system for Alzheimer's disease," Biosens. Bioelectron., vol. 196, pp. 113730, 2022, doi: 10.1016/j.bios.2021.113730.
[4] Y. Wu, X. Ma, K. Li et al., "Bipolar electrode-based sheath-less focusing and continuous acoustic sorting of particles and cells in an integrated microfluidic device," Anal. Chem., vol. 96, no. 8, pp. 3627-3635, 2024, doi: 10.1021/acs.analchem.3c05755.
[5] J. Qian, H. Lan, L. Huang et al., "Acoustofluidics for simultaneous droplet transport and centrifugation facilitating ultrasensitive biomarker detection," Lab Chip, vol. 23, no. 19, pp. 4343-4351, 2023, doi: 10.1039/d3lc00626c.
[6] P. Zhang, C. Chen, F. Guo et al., "Contactless, programmable acoustofluidic manipulation of objects on water," Lab Chip, vol. 19, no. 20, pp. 3397-3404, 2019, doi: 10.1039/c9lc00465c.
[7] S. Yang, Z. Tian, Z. Wang et al., "Harmonic acoustics for dynamic and selective particle manipulation," Nat. Mater., vol. 21, no. 5, pp. 540-546, 2022, doi: 10.1038/s41563-022-01210-8.
[8] Z. Wang, J. Rich, N. Hao et al., "Acoustofluidics for simultaneous nanoparticle-based drug loading and exosome encapsulation," Microsyst. Nanoeng., vol. 8, no. 1, pp. 45, 2022, doi: 10.1038/s41378-022-00374-2.
[9] C. Sun, R. Mikhaylov, Y. Fu et al., "Flexible printed cir-cuit board as novel electrodes for acoustofluidic devices," IEEE Trans. Electron Devices, vol. 68, no. 1, pp. 393-398, 2020, doi: 10.1109/TED.2020.3039760.
[10] C. Sun, R. Mikhaylov, X. Yang et al., "Enhanced integrated acoustoflu-idics with printed circuit board electrodes attached to piezoelectric film coated substrate," Ultrasonics, vol. 147, pp. 107531, 2025, doi: 10.1016/j.ultras.2024.107531.
[11] S. Han, T. Wu, H. Li et al., "Dual-wave hybrid acoustofluidic cen-trifuge for rapid enrichment of micro-and nanoscale biological par-ticles," Sens. Actuators A, Phys., vol. 389, pp. 116495, 2025, doi: 10.1016/j.sna.2025.116495.
[12] M. Stringer, P. Dumcius, X. Zhang et al., "Multidirectionally patterned interdigital transducers for enhancing acoustofluidic streaming with flexible printed circuit board," Adv. Funct. Mater., pp. 2421308, 2025, doi: 10.1002/adfm.202421308.
[13] C. Sun, F. Wu, D. Wallis et al., "Gallium nitride: a versatile compound semiconductor as novel piezoelectric film for acoustic tweezer in ma-nipulation of cancer cells," IEEE Trans. Electron Devices, vol. 67, no. 8, pp. 3355-3361, 2020, doi: 10.1109/TED.2020.3002498.
[14] C. Zhang, N. Rong, Z. Lin et al., "Acoustic enrichment of sperm for in vitro fertilization," Lab Chip, vol. 24, no. 22, pp. 5113-5123, 2024, doi: 10.1039/D4LC00604F.